Wannier-Stark states in double-periodic lattices. I. One-dimensional lattices

Dmitrii N. Maksimov,[1] Evgeny N. Bulgakov,[1,2] and Andrey R. Kolovsky[1,3]
[1]*Kirensky Institute of Physics, 660036 Krasnoyarsk, Russia*
[2]*Siberian State Aerospace University, 660014 Krasnoyarsk, Russia*
[3]*Siberian Federal University, 660041 Krasnoyarsk, Russia*
(Received 25 November 2014; published 28 May 2015)

We analyze the Wannier-Stark spectrum of a quantum particle in generic one-dimensional double-periodic lattices. In the limit of a weak static field, the spectrum is shown to be a superposition of two Wannier-Stark ladders originating from two Bloch subbands. As the strength of the field is increased, the spectrum rearranges itself into a single Wannier-Stark ladder. We derive analytical expressions that describe the rearrangement employing the analogy between the Wannier-Stark problem and a driven two-level system in the strong-coupling regime.

DOI: 10.1103/PhysRevA.91.053631 PACS number(s): 03.75.Lm, 73.22.Dj, 05.60.Gg

I. INTRODUCTION

By definition, Wannier-Stark (WS) states are the eigenstates of a quantum particle in a periodic potential in the presence of a static field F. For a simple one-dimensional (1D) lattice of period a the spectrum of WS states is a ladder of energy levels with the level spacing aF, known as the Wannier-Stark ladder or the Wannier-Stark fan. The equidistant spectrum implies periodic dynamics of the particle, which is simply the celebrated Bloch oscillations (BOs). If the lattice period is doubled, BOs become a complicated process because of the Landau-Zener (LZ) tunneling between two subbands that emerge from a single band. In the past decade BOs and LZ tunneling in 1D double-periodic lattices have attracted much attention in cold-atoms physics and photonics due to applications in interferometric measurements and as a method for manipulating localized wave packets [1–5]. We mention that these phenomena were analyzed earlier in the context of solid-state systems, where the considered model was a crystal with two minibands subject to an electric field [6–10].

The main question we address in this work is how the interband LZ tunneling is encoded in the properties of WS states. In fact, since an arbitrary initial quantum state of the system can be expanded over the basis of WS states, they provide an alternative approach for describing various dynamical phenomena, including LZ tunneling. The advantage of this alternative approach becomes especially transparent in two-dimensional systems, which will be the subject of the following paper [11]. Thus the present work can be also viewed as a necessary step before proceeding with analysis of WS states in two-dimensional lattices.

The structure of the paper is as follows. In Sec. II we introduce the model, the tight-binding Hamiltonian of a double-periodic lattice, and perform a preliminary analysis of the Wannier-Stark spectrum. The analysis reveals two different regions in the parameter space: the cases of weak and strong fields, which are studied in detail in Sec. III. We obtain asymptotic expressions for the WS spectrum in the limit $F \to \infty$ and $F \to 0$ and discuss two analytical methods that describe this spectrum for intermediate F. Finally, in Sec. IV we analyze the system beyond the tight-binding approximation. The main results are summarized in Sec. V.

II. MODEL

Within the tight-binding approximation an arbitrary double-periodic lattice is characterized by four parameters: alternating tunneling elements J_1 and J_2, alternating on-site energies $\pm\delta$, and the Stark energy aF. Thus, in the second quantized form the Hamiltonian reads

$$H = -J_1 \sum_{m\ \mathrm{odd}} (c^\dagger_{m+1} c_m + \mathrm{H.c.}) - J_2 \sum_{m\ \mathrm{even}} (c^\dagger_{m+1} c_m + \mathrm{H.c.}) + \delta \sum_m (-1)^m c^\dagger_m c_m + aF \sum_m (m - 1/2) c^\dagger_m c_m, \qquad (1)$$

where the last term corresponds to the potential energy $F(x - x_0)$ with x_0 chosen in the middle between two sites. For $F = 0$ the single-particle spectrum of the system (1) consists of two Bloch bands

$$E_\pm(\kappa) = \pm\sqrt{\delta^2 + J_1^2 + J_2^2 + 2J_1 J_2 \cos(2\kappa)}, \qquad (2)$$

where κ is the quasimomentum defined in the reduced Brillouin zone $-\pi/2 \leqslant \kappa < \pi/2$ (we set the distance a between the nearest sites to unity). In what follows we will be mainly concerned with two cases: (i) $J_1 = J_2 \equiv J$ and $\delta \neq 0$ and (ii) $\delta = 0$ and $J_1 \neq J_2$. These two lattices may have almost indistinguishable Bloch spectra [see Fig. 1(a)], however, their Bloch states are profoundly different. In fact, the Bloch states of lattice (ii), known in solid-state physics as the Su-Schrieffer-Heeger (SSH) lattice [12], possess nontrivial topological properties reflected in the quantized Zak phase [13]. In contrast, case (i) corresponds to a topologically trivial lattice. We mention in passing that recently the Zak phase was measured in the cold-atom implementation of the model (1) in Ref. [14].

If $F \neq 0$ the continuous Bloch spectrum (2) transforms into the discrete WS spectrum. For the sake of preliminary analysis we calculate the spectrum using the straightforward diagonalization of the Hamiltonian matrix. Denoting probability amplitudes for the odd and even sites $\psi_l^{A,B}$ (here index l labels elementary cell consisting of two sites), we have the stationary Schrödinger equation in the form

$$\begin{aligned} 2F(l - 1/4)\psi_l^A - \delta\psi_l^A - J_2\psi_l^B - J_1\psi_{l-1}^B &= E\psi_l^A, \\ 2F(l + 1/4)\psi_l^B + \delta\psi_l^B - J_2\psi_l^A - J_1\psi_{l+1}^A &= E\psi_l^B. \end{aligned} \qquad (3)$$

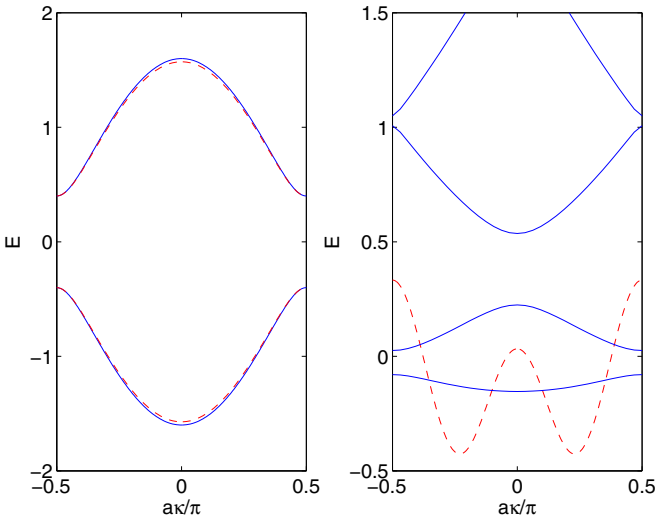

FIG. 1. (Color online) Shown on the left are Bloch bands of the tight-binding system (1) for $J = 0.76$ and $\delta = 0.4$ (dashed line) and for $J_1 = 1$, $J_2 = 0.6$, and $\delta = 0$ (solid line). In what follows, these two sets of parameters are referred to as lattice (i) and lattice (ii), respectively. The constants J_1, J_2, δ, and the energy E are measured in arbitrary energy units. Shown on the right is the Bloch spectrum of the continuous system (39), which will be discussed in Sec. IV. The distance a between the nearest sites is set to unity in the subsequent figures.

The solid lines in Fig. 2 show the numerical solution of Eq. (3) as a function of F for lattice (ii). It can be seen that the spectrum consists of two Wannier-Stark fans that are associated with two Bloch bands in Fig. 1(a). In the region of large F the ladders strongly affect each other, which is reflected in pronounced avoided crossings. The size of the avoided crossings, however, progressively decreases if $F \to 0$. This can be clearly seen in

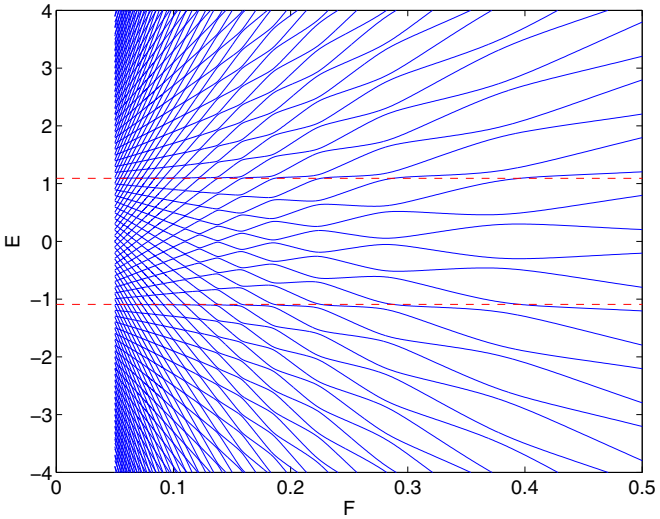

FIG. 2. (Color online) Wannier-Stark spectrum for lattice (ii) as a function of the Stark energy aF. The dashed lines correspond to Eq. (4) with $n = 0$. These lines indicate the origins of two intersecting Wannier-Stark fans and illustrate the meaning of the geometric phase discussed in Sec. III B.

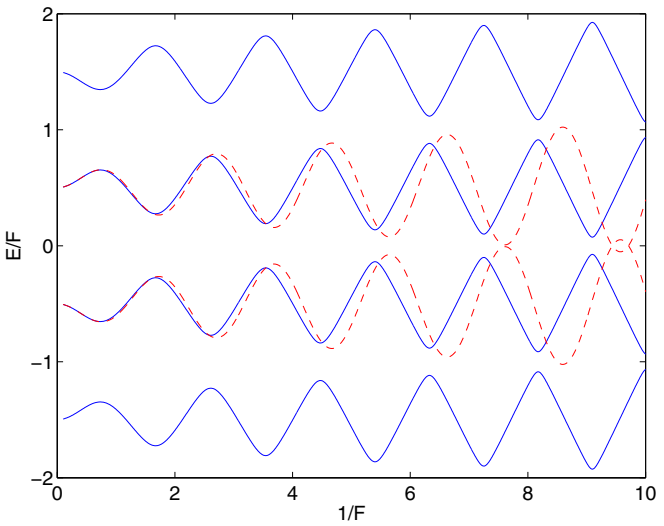

FIG. 3. (Color online) Scaled spectrum as a function of $1/F$. Solid lines are the four nearest $E = 0$ energy levels from Fig. 2. The dashed lines are analytical result for the Wannier-Stark spectrum in the strong-field limit [see Eq. (28) in Sec. III A].

Fig. 3, where we scale the spectrum according to the ladder spacing F. Thus, in the limit of small F we have

$$E_{n,\pm} \approx \pm C + 2Fn, \quad n = 0, \pm 1, \ldots, \tag{4}$$

where the constant C will be specified later on in Sec. III B. It can also be seen in Fig. 3 that in the opposite limit of large F two Wannier-Stark ladders merge into one ladder with the level spacing F, i.e.,

$$E_n \approx F(n + 1/2), \quad n = 0, \pm 1, \ldots. \tag{5}$$

To calculate the spectrum using Eq. (3) we truncate an infinite system of equations to a finite system, which results in numerical errors. In the next section we describe an approach that is free from this drawback and more importantly opens a way for finding analytical solutions.

III. FLOQUET OPERATOR APPROACH

To approach Eq. (3) analytically we introduce the generating functions

$$Y^{A,B}(\theta) = (2\pi)^{-1/2} \sum_{l=-\infty}^{\infty} \psi_l^{A,B} \exp(il\theta). \tag{6}$$

This reduces Eq. (3) to the system of two ordinary differential equations

$$i2F \frac{d\mathbf{Y}(\theta)}{d\theta} = G(\theta)\mathbf{Y}(\theta), \tag{7}$$

where $\mathbf{Y}(\theta) = [Y^A(\theta), Y^B(\theta)]$ and the 2×2 matrix $G(\theta)$ is given by

$$G(\theta) = \begin{pmatrix} E + F/2 + \delta & J_2 + J_1 \exp(-i\theta) \\ J_2 + J_1 \exp(i\theta) & E - F/2 - \delta \end{pmatrix}. \tag{8}$$

Since $Y^{A,B}(\theta)$ are by definition periodic functions of θ, we are only interested in periodic solutions of Eq. (7). This

gives the quantization rule for the energy E entering Eq. (8). The periodicity of solutions implies that eigenvalues of the evolution (Floquet) operator

$$U = \widehat{\exp}\left[-\frac{i}{2F}\int_0^{2\pi} G(\theta)d\theta\right] \tag{9}$$

must be unity. Numerically, we can use this fact to find the Wannier-Stark spectrum exactly, i.e., without using the truncation procedure. In more detail, first we calculate (9) for a trial energy $E = 0$ and diagonalize it. This provides two complex eigenvalues λ_1 and $\lambda_2 = \lambda_1^*$. Then the positions of energy levels in Figs. 2 or 3 are found from the equation

$$\exp\left(-i\frac{\pi E}{F}\right) = \lambda_{1,2}. \tag{10}$$

Unfortunately, Eq. (7) has no analytical solution in the closed form that would be valid in the whole parameter space. Nevertheless, we can obtain an analytical solution in the case of weak fields and separately in the case of strong fields. A quantity that distinguishes these two cases is obviously the size of the energy gap separating two Bloch subbands as compared to the Stark energy. In terms of Bloch dynamics it distinguishes the regime of negligible interband LZ tunneling from that where the tunneling is the main effect. We begin with the case of strong fields.

A. Strong fields

As it was already mentioned in Sec. II, in the limit of large F two ladders are strongly coupled, which leads to an almost equidistant spectrum with the level spacing F. The parameters that quantify the strength of coupling are

$$\epsilon_1 = (J_2 - J_1)/F \tag{11}$$

if $\delta = 0$ and

$$\epsilon_2 = \delta/F \tag{12}$$

if $J_1 = J_2$ but $\delta \neq 0$. The maximal coupling corresponds to $\epsilon_1 = 0$ ($\epsilon_2 = 0$), which is reached either by taking the limit $F \to \infty$ or by closing the energy gap between Bloch subbands. In terms of Eq. (7) this corresponds to the trivial solutions

$$\mathbf{Y}_-(\theta) = \frac{1}{\sqrt{2\pi}}\begin{pmatrix} e^{in\theta} \\ 0 \end{pmatrix}, \quad \mathbf{Y}_+(\theta) = \frac{1}{\sqrt{2\pi}}\begin{pmatrix} 0 \\ e^{in\theta} \end{pmatrix}, \tag{13}$$

with the energies $E_{n,+}=F(2n+1/2)$ and $E_{n,-}=F(2n-1/2)$, respectively. To find the periodic solutions of Eq. (7) for finite ϵ_1 and/or ϵ_2 we use (and compare) two different methods: the Wu-Yang iterative approach from the theory of periodically driven two-level systems [15] and a perturbative approach based on the Bogoliubov-Mitropolskii averaging technique from the theory of classical dynamical systems [16].

1. *Wu-Yang iterative approach*

Let us consider lattice (i), i.e., $J_1 = J_2 \equiv J$ and $\delta \neq 0$. After the substitution

$$\begin{aligned} Y^A &= \tilde{Y}^A \exp(-iE\theta/2F - i\theta/4), \\ Y^B &= \tilde{Y}^B \exp(-iE\theta/2F + i\theta/4) \end{aligned} \tag{14}$$

and $t = \theta/2$, Eq. (7) takes the form of the Schrödinger equation for a periodically driven two-level system

$$i\frac{d}{dt}\begin{pmatrix} \tilde{Y}^A \\ \tilde{Y}^B \end{pmatrix} = \begin{pmatrix} \epsilon_2 & \Omega\cos t \\ \Omega\cos t & -\epsilon_2 \end{pmatrix}\begin{pmatrix} \tilde{Y}^A \\ \tilde{Y}^B \end{pmatrix}, \tag{15}$$

where $\Omega = 2J/F$ plays the role of the Rabi frequency. Since we are interested in the limit $\epsilon_2 \ll \Omega$ we are in the so-called strong-coupling regime where the common rotating-wave approximation is not justified. This regime has attracted much attention in quantum optics; we will follow the above-cited work [15], which reports recent progress in the strong-coupling problem. Essentially the method provides an approximate expression for the evolution operator $U(t)$,

$$\tilde{\mathbf{Y}}(t) = U(t)\tilde{\mathbf{Y}}(0), \tag{16}$$

which is given in the Appendix. To satisfy the periodicity of the solutions, Eq. (16) should be complemented with the boundary conditions

$$\begin{aligned} \tilde{Y}^A(\pi) &= \exp\left(-i\frac{E\pi}{F}\right)\tilde{Y}^A(0), \\ \tilde{Y}^B(\pi) &= -\exp\left(-i\frac{E\pi}{F}\right)\tilde{Y}^B(0). \end{aligned} \tag{17}$$

This yields the spectrum

$$E_{n,\pm} = F(2n \pm 1/2) \pm \frac{F}{\pi}\arcsin\left(\frac{U_{11}(\pi) - U_{22}(\pi)}{2i}\right), \tag{18}$$

where $U_{11}(t)$ and $U_{22}(t)$ are the diagonal elements of the evolution operator in Eq. (16). Expanding Eq. (18) in the parameter $\epsilon \equiv \epsilon_2$ up to fourth order, we have

$$E_{n,\pm} = F(2n \pm 1/2) \pm \epsilon\Pi_1(F) \pm \epsilon^3\Pi_3(F), \tag{19}$$

where

$$\Pi_1(F) = F\mathcal{J}_0\left(\frac{4J}{F}\right) \tag{20}$$

and

$$\begin{aligned} \Pi_3(F) = \frac{2F}{\pi}\int_0^{\pi} dt\left[\mathcal{I}\left(t,\frac{4J}{F}\right) - \frac{1}{2}\mathcal{I}\left(\pi,\frac{4J}{F}\right)\right]^2 \\ \times \cos\left(\frac{4J}{F}\sin t\right). \end{aligned} \tag{21}$$

In these last two equations $\mathcal{J}_0(z)$ is the Bessel function of the first kind and

$$\mathcal{I}(t,z) = \int_0^t dx\,\sin(z\sin x). \tag{22}$$

The accuracy of the asymptotic equation (19) is illustrated in Fig. 4. In this figure the solid lines are the exact spectrum calculated by using Eqs. (9) and (10), the dashed lines the first-order corrections to the zeroth-order result, and the dash-dotted lines the third-order corrections. It can be seen in Fig. 4(a) that the first-order result systematically shifts positions of the avoided crossings. This is corrected by the third-order term in Eq. (19); now the avoided crossings appear at the right positions. Unfortunately, applicability of Eq. (19) is restricted to small ϵ and if δ is increased, this automatically decreases the validity interval in F [see Fig. 4(b)]. In this figure we also depict the result according to Eq. (18). It can be seen in

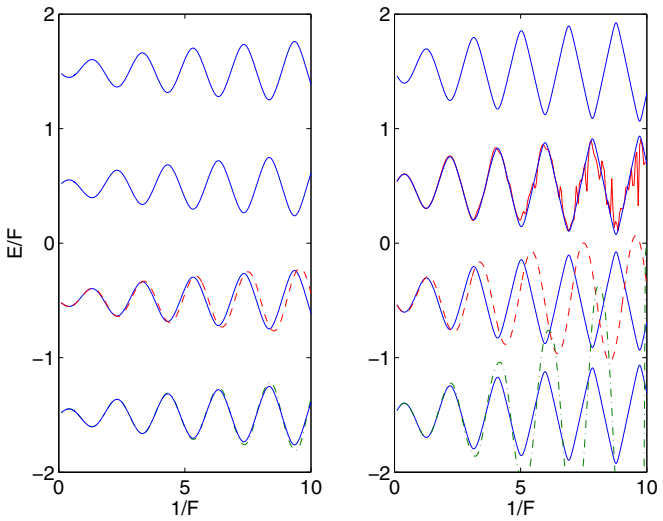

FIG. 4. (Color online) Scaled spectrum for lattice (i) with $J_1 = J_2 = 0.76$ and $\delta = 0.2$ (left) and $\delta = 0.4$ (right). The dashed and dash-dotted lines are the first- and third-order approximations according to Eq. (19), respectively, and the broken line corresponds to Eq. (18).

Fig. 4(b) that Eq. (18) removes the divergence of Eq. (19) but introduces unphysical oscillations.

2. *Bogoliubov-Mitropolskii averaging technique*

Next we discuss the perturbative approach based on the Bogoliubov-Mitropolskii averaging technique [16]. In this section we consider the general case $\delta \neq 0$ and $J_1 \neq J_2$. Let us rewrite Eq. (7) in terms of the parameters in Eqs. (11) and (12). This is done by using two substitutions. The first substitution defined in Eq. (14) results in the equation

$$i2F\frac{d}{d\theta}\begin{pmatrix}\tilde{Y}^A\\ \tilde{Y}^B\end{pmatrix} = \begin{pmatrix}\delta & g(\theta)\\ g^*(\theta) & -\delta\end{pmatrix}\begin{pmatrix}\tilde{Y}^A\\ \tilde{Y}^B\end{pmatrix}, \tag{23}$$

where $g(\theta) = J_1\exp(i\theta/2) + J_2\exp(-i\theta/2)$. The second substitution is

$$u = (\tilde{Y}^A + \tilde{Y}^B)\exp\left(-\frac{i}{2F}\int \mathrm{Re}[g]d\theta\right),$$
$$v = (\tilde{Y}^A - \tilde{Y}^B)\exp\left(+\frac{i}{2F}\int \mathrm{Re}[g]d\theta\right). \tag{24}$$

This gives

$$i\frac{d}{d\theta}\begin{pmatrix}u\\ v\end{pmatrix} = \begin{pmatrix}0 & f(\theta)\\ f^*(\theta) & 0\end{pmatrix}\begin{pmatrix}u\\ v\end{pmatrix}, \tag{25}$$

where

$$f(\theta) = \left[\epsilon_2 + i\epsilon_1\sin\left(\frac{\theta}{2}\right)\right]\exp\left[i\frac{2(J_1+J_2)}{F}\sin\left(\frac{\theta}{2}\right)\right]. \tag{26}$$

Since the function $f(\theta)$ is proportional to small parameters ϵ_1 and/or ϵ_2, Eq. (25) can be treated by the Bogoliubov-Mitropolskii perturbative approach.

The first order of the Bogoliubov-Mitropolskii theory amounts to replacing the function $f(\theta)$ in Eq. (25) by its mean value

$$\bar{f} = \frac{\delta}{F}\mathcal{J}_0\left(\frac{2(J_1+J_2)}{F}\right) + \frac{J_1-J_2}{F}\mathcal{J}_1\left(\frac{2(J_1+J_2)}{F}\right), \tag{27}$$

where $\mathcal{J}_0(z)$ and $\mathcal{J}_1(z)$ are the Bessel functions of the first kind. After the above substitution Eq. (25) is trivially solved, providing two independent solutions. Next, using the substitutions (14) and (24) in the reverse order, we find two independent approximate solutions of Eq. (7). Finally, requiring that these solutions are periodic in θ, we obtain corrections to the equidistant spectrum

$$E_{n,\pm} = F\left[2n \pm \tfrac{1}{2} \pm \bar{f}(F)\right]. \tag{28}$$

If $J_1 = J_2$ this result coincides with the first-order corrections obtained in the previous section. In the case $J_1 \neq J_2$, i.e., for lattice (ii), the approximate solution (28) is depicted in Fig. 3 by the dashed lines. Notice a different asymptotic behavior at $1/F \to 0$ as compared to lattice (i).

Comparing two methods used in this work, we conclude that both methods give a tractable analytical expression only in the first order over the perturbative parameter. Furthermore, when restricted to first order, the Bogoliubov-Mitropolskii technique is simpler and more universal than the Wu-Yang approach.

B. Weak-field regime

1. *Geometric phase and asymptotic solution*

We proceed with the weak-field limit where we shall focus on lattice (ii). Assuming that F is beyond the vicinity of the avoided crossings, the periodic solution of Eq. (7) can be found with the help of the adiabatic theorem. It expresses the function $\mathbf{Y}(\theta) = [Y^A(\theta), Y^B(\theta)]^T$ in terms of instantaneous eigenfunctions $\mathbf{y}_{1,2}(\theta)$ of the 2×2 matrix $G(\theta)$ [Eq. (8)],

$$G(\theta)\mathbf{y}_\pm(\theta) = \mathcal{E}_\pm(\theta)\mathbf{y}_\pm(\theta). \tag{29}$$

We have

$$\mathbf{Y}_\pm(\theta) = e^{-i\Phi_d(\theta)}e^{-i\Phi_g(\theta)}\mathbf{y}_\pm(\theta), \tag{30}$$

where

$$\Phi_d(\theta) = \frac{1}{2F}\int_0^\theta \mathcal{E}_\pm(\theta')d\theta',$$
$$\Phi_g(\theta) = i\int_0^\theta \mathbf{y}_\pm^T(\theta')\frac{d}{d\theta'}\mathbf{y}_\pm(\theta')d\theta' \tag{31}$$

are the dynamical and geometric phases, respectively. It is easy to prove that the eigenvalues $\mathcal{E}_\pm(\theta)$ are given by

$$\mathcal{E}_\pm(\theta) = E + \tilde{\mathcal{E}}_\pm(\theta),$$
$$\tilde{\mathcal{E}}_\pm(\theta) = \pm\sqrt{\left(\delta + \frac{F}{2}\right)^2 + J_1^2 + J_2^2 + 2J_1J_2\cos(\theta)}. \tag{32}$$

To ensure periodicity the solution (30) must satisfy the condition $\Phi_d(2\pi) + \Phi_g(2\pi) = 2\pi n$, where n is an integer. This results in the spectrum

$$E_{n,\pm} = C_\pm + 2F(n + c_\pm), \tag{33}$$

where

$$C_\pm = \frac{1}{2\pi}\int_0^{2\pi}\tilde{\mathcal{E}}_\pm(\theta)d\theta, \quad c_\pm = \frac{i}{2\pi}\int_0^{2\pi}\mathbf{y}_\pm^T(\theta)\frac{d}{d\theta}\mathbf{y}_\pm(\theta)d\theta'. \tag{34}$$

Comparing Eq. (32) with the Bloch dispersion relation (2), we conclude that in the limit of small F the constants $C_\pm$ are given

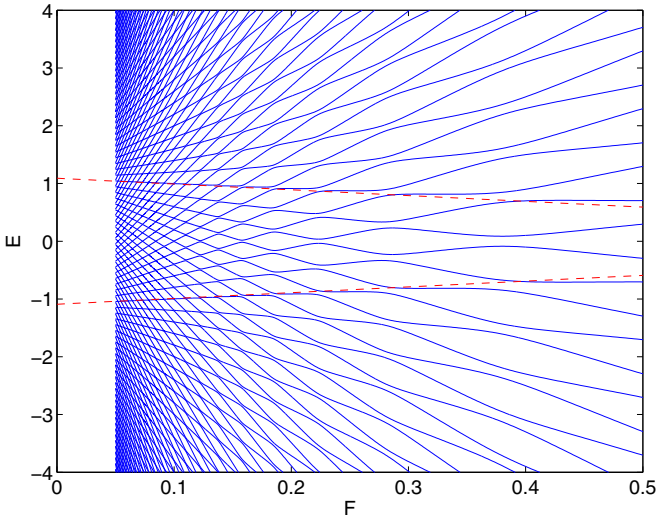

FIG. 5. (Color online) Same as in Fig. 2 but for different dimerization $(J_1, J_2) = (0.6, 1)$. This dimerization has a different geometric phase, which is reflected in the different slope of the dashed lines as compared to Fig. 2.

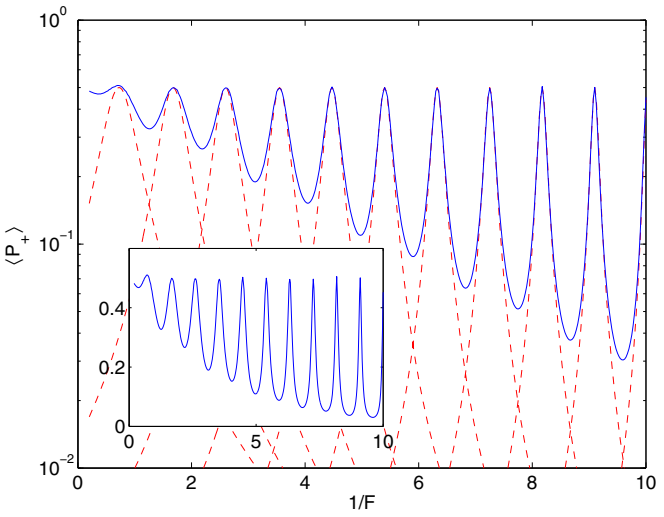

FIG. 6. (Color online) Time-averaged population of the upper band for lattice (ii) as a function of $1/F$ on logarithmic (main panel) and linear (inset) scales. The average is over 40 Bloch periods. (For an infinite number of Bloch periods the hight of all peaks is exactly 1/2.) The dashed lines are approximations of the resonance peaks by the Lorentzian (38).

by the mean energies of the Bloch subbands

$$\lim_{F\to 0} C_{\pm} = \frac{1}{\pi}\int_{-\pi/2}^{\pi/2} E_{\pm}(\kappa)d\kappa, \quad C_{+} = -C_{-} \equiv C \tag{35}$$

and the constants $c_{\pm}$ are the Zak phases of these bands. For the example considered in Fig. 2 $c_{\pm} = 0$ and hence we recover Eq. (4). However, for the alternative dimerization of the SSH lattice $J_2 \leftrightarrow J_1$, one has $c_{\pm} = \pm 1/2$ and Eq. (4) must be corrected as $E_{n,\pm} = \pm C + 2F(n \pm 1/2)$. The WS spectrum of lattice (ii) for the alternative dimerization is depicted in Fig. 5. Because the system dynamics is determined by transition frequencies between energy levels, Fig. 5 describes the same physical situation as in Fig. 2. However, formally the spectrum does depend on the lattice dimerization, which is reflected in Eq. (33). As it was already mentioned in Sec. II, the SSH lattice is a topological system, i.e., its geometric phase is insensitive to variation of the tunneling rates and is either zero ($J_2 < J_1$) or $\pm 1/2$ ($J_2 > J_1$). This result does not hold in the topologically trivial case $\delta \neq 0$ where the constants $c_{\pm}$ in Eq. (33) depend on the tunneling rates and in principle can take arbitrary values.

The accuracy of the adiabatic equation (33) can be improved by including the second-order corrections that are proportional to F^2. Using the analogy with spin-1/2 dynamics and adopting results of Ref. [17] to the problem under consideration, the coefficient in front of F^2 is found as

$$D = \frac{(J_1+J_2)^2(J_1-J_2)^2}{32}\frac{1}{2\pi}\int_0^{2\pi}[(J_1+J_2)^2\cos^2(\theta/2) + (J_1-J_2)^2\sin^2(\theta/2)]^{-5/2}d\theta. \tag{36}$$

2. *Avoided crossings and resonant tunneling*

An important point requiring special attention is that the adiabatic equation (33) breaks down at the level crossings. Here the level crossings should be replaced with avoided crossings with the gap ΔE. Drawing an analogy with the driven two-level system, where the avoided crossings are associated with multiphoton resonances [18], we have

$$\frac{\Delta E}{F} = \frac{2}{\pi}\exp\left(-\frac{1}{F}\int_0^{\theta_0}\sqrt{1-\frac{2J_1J_2}{J_1^2+J_2^2}\cosh(\theta)}d\theta\right), \quad \frac{2J_1J_2}{J_1^2+J_2^2}\cosh(\theta_0) = 1. \tag{37}$$

It is easy to show that the avoided crossings between Wannier-Stark levels describe the so-called phenomenon of the resonant LZ tunneling. This phenomenon can be detected by analyzing population dynamics of the Bloch subbands [8,10]. In fact, let us assume that initially the system is in the ground state and consider the time-averaged occupation of the upper band $P_+ = \langle P_+(t)\rangle$ as a function of the static field. For lattice (ii) the result of this experiment is depicted in Fig. 6. This figure should be compared with Fig. 3. It can be seen that positions of the resonance peaks coincide with the positions of the avoided crossings in Fig. 3, while the widths of the peaks are determined by the gaps ΔE_j, so locally one has

$$P_+(z) = 0.5\frac{(\Delta E_j/2)^2}{(\Delta E_j/2)^2 + (z-z_j)^2}, \quad z = \frac{1}{F}. \tag{38}$$

An interesting dynamical manifestation of the resonant tunneling is a possibility of transferring the quantum particle from the lower Bloch subband to the upper subband and vice versa. Assume that F is not near a given avoided crossing and the initial state of the system is a wave packet constructed from Bloch states belonging to the lower subband. Then the particle performs BOs in the lower subband with negligible LZ tunneling to the upper subband. If we now adiabatically change F to pass through the avoided crossing, the particle will perform BOs in the upper subband. This dynamics is illustrated in Fig. 7, which shows BOs of a localized packet. In this simulation we linearly change F in the

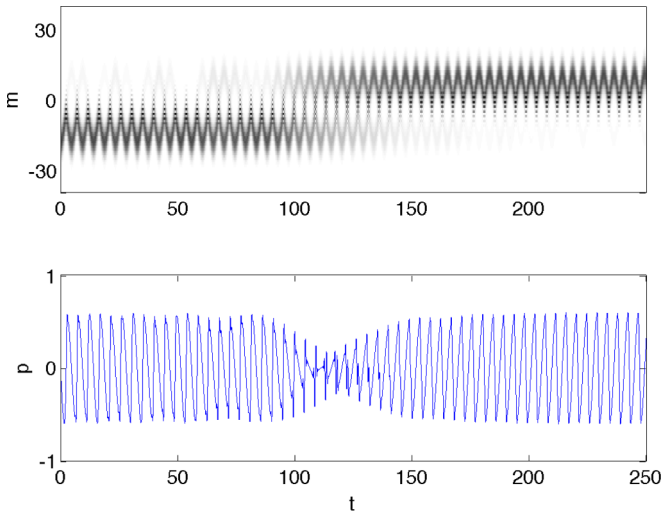

FIG. 7. (Color online) Dynamics of a localized wave-packet (top) and the mean momentum (bottom) as functions of time. The initial condition corresponds to a Gaussian wave packet of a width of approximately five sites located at $m = -20$. Within the considered time interval the static force is linearly increased from $F = 1/9.4$ to $F = 1/8.7$. The other parameters are the same as in Fig. 6. The time is measured in units of $T_J = 2\pi/J_1$ and the momentum in units of $\hbar/a$.

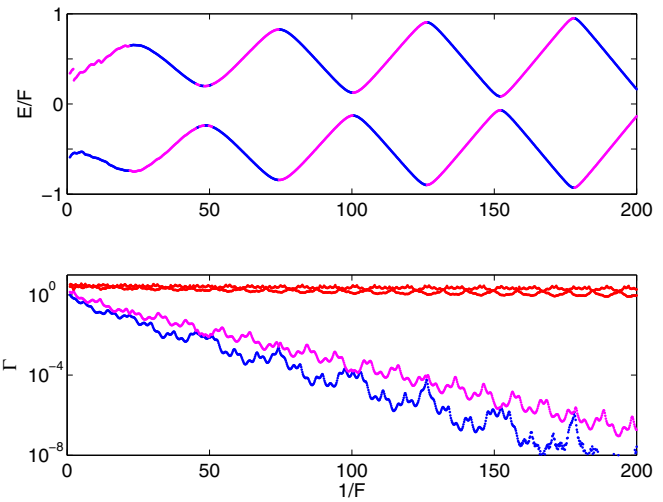

FIG. 8. (Color online) Level positions (top) and their widths (bottom) for two stable Wannier-Stark ladders originating from the first and second Bloch bands in Fig. 1(b). Two additional upper curves in the bottom panel are the level widths for unstable Wannier-Stark ladders originating from the third and fourth Bloch bands.

interval $8.7 < 1/F < 9.4$, which contains one avoided crossing at $1/F \approx 9$ (see Fig. 3).

We conclude this section with a remark concerning future prospects. Nowadays, in cold-atom physics much attention is paid to atom-atom interactions. With respect to the interband LZ tunneling, the role of interactions is discussed, for example, in Refs. [19–23]. The cited papers analyze the nonlinear dynamics of the system in terms of the Gross-Pitaevskii equation or the discrete nonlinear Schrödinger equation. The main effects found are the broadening of resonance peaks and asymmetry of the tunneling. It would be interesting to look for *stationary* solutions of Eq. (3) complemented by nonlinear terms.

IV. BEYOND THE TIGHT-BINDING APPROXIMATION

In this section we discuss the cold-atom implementation of double-periodic lattices considered in the previous sections. After an appropriate rescaling, the dimensionless Hamiltonian of the system reads

$$\widehat{H} = -\frac{1}{2}\frac{d^2}{dx^2} + V(x) + Fx,$$
$$V(x) = V_0 + V_1\cos(2\pi x + \phi_1) + V_2\cos(4\pi x + \phi_2), \quad (39)$$

where V_1 and V_2 are proportional to the intensities of two standing laser waves forming the optical lattice [4,14]. For numerical purposes we introduce an additional parameter V_0 in the Hamiltonian (39) to shift the energy axis. Varying the parameters of the double-periodic potential $V(x)$, one can realize different values of the hopping matrix elements J_1 and J_2 and on-site energy $\pm\delta$ in the tight-binding model. In what follows we set $\phi_1 = \phi_2 = 0$, which ensures $\delta = 0$, and $|V_1| < |V_2|$, which ensures $J_2 < J_1$, and consider relatively small V_2, which implies a shallow lattice. As an example, Fig. 1(b) shows the Bloch spectrum of the system (39) for $(V_0, V_1, V_2) = (-0.117, -0.15, 0.3)$. In this figure we also depict by the dashed line the potential $V(x)$. Our prime interest in Fig. 1(b) is two lower bands with the gap controlled by the parameter V_1. (Notice that for $V_1 = 0$ the gap closes.) We stress that we intentionally consider a shallow lattice because it justifies our model (1). If the lattice were deeper one must take into account the next two bands, which would essentially complicate the tight-binding model.

If $F \neq 0$ every Bloch band in Fig. 1(b) originates a Wannier-Stark ladder with an equidistant spectrum. (For neutral atoms the static force is typically introduced by accelerating the lattice or by using a nonuniform magnetic field with constant gradient.) However, unlike the tight-binding model, the energy levels are now complex numbers

$$E'_{n,\alpha} = E_{n,\alpha} + i\Gamma_\alpha \quad (40)$$

(here α is the band index) and the associated WS states are metastable states (quantum resonances) with a finite lifetime that is inversely proportional to the resonance width Γ_α [24]. Of course, only long-living WS states are of physical importance. The energies of these states, reduced to the fundamental energy interval $|E| \leqslant F/2$, are shown in the top panel in Fig. 8. This figure should be compared with Fig. 3, where one can see a similar structure with progressively decreasing size of the avoided crossings. We note that, even if an avoided crossing is not resolved on the scale of the figure, we can detect its presence by sorting the levels according to their stability. In fact, if the real parts of the complex energy levels undergo an avoided crossing, the imaginary parts must cross [24]. This behavior can be clearly observed in Fig. 8(b), where the ladders exchange their stability at the avoided crossings.

As expected, we find the strongest deviation of the original system from its tight-binding counterpart in the limit of strong fields. In this domain coupling with higher ($\alpha > 2$) Bloch

bands results in nonanalytic behavior of $E_{n,\pm} = E_{n,\pm}(F)$, which is seen as discontinuity of the curves in Fig. 8(a). Nevertheless, the above conclusion that two Wannier-Stark ladders merge into a single ladder in the limit $F \to \infty$ remains valid.

Here it is also appropriate to discuss another approximation of the continuous system (39) known as the two-band model [6]:

$$H = \sum_l [(\delta_a + 2Fl)a_l^\dagger a_l - \tilde{J}_a(a_{l+1}^\dagger a_l + \text{H.c.})] + \sum_l [(\delta_b + 2Fl)b_l^\dagger b_l + \tilde{J}_b(b_{l+1}^\dagger b_l + \text{H.c.})] + \tilde{J}_{ab} F \sum_l (b_l^\dagger a_l + \text{H.c.}). \quad (41)$$

In this Hamiltonian the first and second terms explicitly refer to the first and second bands in Fig. 1(b) and the last term is the interband coupling induced by the static field. Notice that that the summation index l refers to the lattice cells but not the lattice sites. The model (41) captures essentially the same physics as the model (1) and, in principle, the parameters of the Hamiltonian (41) can be related to those of the Hamiltonian (1). In the present work we prefer to stay with the model (1) because of advantages in the analytical treatment of the WS spectrum and because laboratory experiments with cold atoms and photonics crystal provide numerical values for the parameters of the model (1).

V. CONCLUSION

We analyzed the energy spectrum of a quantum particle in a 1D double-periodic lattice in the presence of a static field F. It was shown that in the limit of weak fields the spectrum consists of two Wannier-Stark ladders originating from two Bloch subbands. Each of these ladders is proved to be uniquely characterized by two parameters: the mean energy and geometric (Zak) phase of the Bloch subbands. An additional characteristic of the spectrum is the size of avoided crossings between energy levels associated with two different ladders. These avoided crossings occur at certain values of F and correspond to resonant interband Landau-Zener tunneling. In the limit $F \to 0$ the size of avoided crossings decreases exponentially with F. In the opposite limit, when F is increased, the energy gaps at avoided crossings progressively increase and sooner or latter become comparable to the ladder step. This results in rearrangement of the spectrum from a superposition of two ladders with the step $2aF$ into a single ladder with the step aF (here a is the distance between the nearest sites). By mapping the problem to an effective two-level system we derived analytic expressions that describe this rearrangement. Remarkably, for the lattice with alternating on-site energies this effective system coincides with the driven two-level system in the strong-coupling regime. Thus we demonstrated that the latter problem, which is of great importance in quantum optics, can be viewed as a particular case of the Wannier-Stark problem for double-periodic lattices.

Finally, we analyzed the Wannier-Stark spectrum of a quantum particle in a double-periodic lattice beyond the tight-binding approximation. The above-listed results were shown to hold true for the original continuous system where the Wannier-Stark states are quantum resonances and hence have a finite lifetime.

ACKNOWLEDGMENTS

The authors acknowledge financial support from Russian Foundation for Basic Research through the Project No. 15-02-00463, Wannier-Stark states and Bloch oscillations of a quantum particle in a generic two-dimensional lattice.

APPENDIX

The solution of Eq. (15) according to the second-order Wu-Yang procedure in Ref. [15] could be written as

$$\tilde{\mathbf{Y}}(t) = U(t)\tilde{\mathbf{Y}}(0), \quad (A1)$$

where $U(t)$ is the 2×2 matrix with elements given by

$$U_{11} = e^{i\beta}([\cos\tau\cos\phi - i\sin\tau\sin\phi]\cos\psi - [i\cos\tau\sin\phi - \sin\tau\cos\phi]\sin\psi),$$
$$U_{12} = e^{-i\beta}([\cos\tau\cos\phi - i\sin\tau\sin\phi]\sin\psi + [i\cos\tau\sin\phi - \sin\tau\cos\phi]\cos\psi),$$
$$U_{21} = e^{i\beta}([\sin\tau\cos\phi + i\cos\tau\sin\phi]\cos\psi - [i\cos\tau\cos\phi + \sin\tau\sin\phi]\sin\psi),$$
$$U_{22} = e^{-i\beta}([\sin\tau\cos\phi + i\cos\tau\sin\phi]\sin\psi + [i\cos\tau\cos\phi + \sin\tau\sin\phi]\cos\psi).$$

The functions $\beta = \beta(t)$, $\tau = \tau(t)$, $\phi = \phi(t)$, and $\psi = \psi(t)$ are defined through the equations

$$\tau(t) = \epsilon\int_0^t dt' \sin[2\Omega\sin t'] = \epsilon\mathcal{I}(t,2\Omega), \quad (A2)$$

$$\beta(t) = \epsilon\int_0^t dt' \cos[2\Omega\sin t']\cos[2\epsilon\mathcal{I}(t',2\Omega)], \quad (A3)$$

$$\phi(t) = -\epsilon\int_0^t dt' \cos[2\Omega\sin t']\sin[2\epsilon\mathcal{I}(t',2\Omega)]\cos\left(2\pi\epsilon\mathcal{J}_0(2\Omega) - 2\epsilon\int_0^{t'} dt'' \sin[2\Omega\cos t'']\right), \quad (A4)$$

$$\psi(t) = \epsilon\int_0^t dt' \cos[2\Omega\sin t']\sin[2\epsilon\mathcal{I}(t',2\Omega)]\sin\left(2\pi\epsilon\mathcal{J}_0(2\Omega) - 2\epsilon\int_0^{t'} dt'' \sin[2\Omega\cos t'']\right). \quad (A5)$$

[1] B. Breid, D. Witthaut, and H. J. Korsch, Bloch-Zener oscillations, New J. Phys. **8**, 110 (2006).
[2] B. Breid, D. Witthaut, and H. J. Korsch, Manipulation of matter waves using Bloch and Bloch-Zener oscillations, New J. Phys. **9**, 62 (2007).
[3] F. Dreisow, A. Szameit, M. Heinrich, T. Pertsch, S. Nolte, A. Tünnermann, and S. Longhi, Bloch-Zener oscillations in binary superlattices, Phys. Rev. Lett. **102**, 076802 (2009).
[4] S. Kling, T. Salger, C. Grossert, and M. Weitz, Atomic Bloch-Zener oscillations and Stückelberg interferometry in optical lattices, Phys. Rev. Lett. **105**, 215301 (2010).
[5] P. Plötz and S. Wimberger, Stückelberg-interferometry with ultra-cold atoms, Eur. Phys. J. D **65**, 199 (2011).
[6] H. Fukuyama, R. A. Bari, and H. C. Fogedby, Tightly bound electrons in a uniform electric field, Phys. Rev. B **8**, 5579 (1973).
[7] X.-G. Zhao, Exact solutions of tightly bound electrons in a uniform electric field: perturbation theory, Phys. Lett. A **154**, 275 (1991).
[8] J. Rotvig, A.-P. Jauho, and H. Smith, Bloch oscillations, Zener tunneling and Wannier-Stark ladders in the time domain, Phys. Rev. Lett. **74**, 1831 (1995).
[9] D. W. Hone and X.-G. Zhao, Time-periodic behavior of multiband superlattices in static electric fields, Phys. Rev. B **53**, 4834 (1996).
[10] X.-G. Zhao, G. A. Georgakis, and Q. Niu, Rabi oscillations between Bloch bands, Phys. Rev. B **54**, R5235 (1996).
[11] D. N. Maksimov, E. N. Bulgakov, and A. R. Kolovsky, Wannier-Stark states in double-periodic lattices II. Two-dimensional lattices, following paper, Phys. Rev. A **91**, 053632 (2015).
[12] W. P. Su, J. R. Schrieffer, and A. J. Heeger, Solitons in polyacetylene, Phys. Rev. Lett. **42**, 1698 (1979).
[13] J. Zak, Berry's phase for energy bands in solids, Phys. Rev. Lett. **62**, 2747 (1989).
[14] M. Atala, M. Aidelsburger, J. T. Barreiro, D. Abanin, T. Kitagawa, E. Demler, and I. Bloch, Direct measurement of the Zak phase in topological bloch bands, Nat. Phys. **9**, 795 (2013).
[15] Y. Wu and X. Yang, Strong-coupling theory of periodically driven two-level systems, Phys. Rev. Lett. **98**, 013601 (2007).
[16] Yu. A. Mitropolskii, *Averaging Methods in Nonlinear Dynamics* (Naukova Dumka, Kiev, 1971) (in Russian).
[17] K. Yu. Bliokh, On spin evolution in a time-dependent magnetic field: Post-adiabatic corrections and geometric phases, Phys. Lett. A **372**, 204 (2008).
[18] V. P. Krainov and V. P. Yakovlev, Quasienergy states of a two-level atom in a strong low-frequency electromagnetic field, Sov. Phys. JETP **51**, 1106 (1980).
[19] M. Jona-Lasinio, O. Morsch, M. Cristiani, N. Malossi, J. H. Müller, E. Courtade, M. Anderlini, and E. Arimondo, Asymmetric Landau-Zener tunneling in a periodic potential, Phys. Rev. Lett. **91**, 230406 (2003).
[20] V. V. Konotop, P. G. Kevrekidis, and M. Salerno, Landau-Zener tunneling of Bose-Einstein condensates in an optical lattice, Phys. Rev. A **72**, 023611 (2005).
[21] S. Wimberger, R. Mannella, O. Morsch, E. Arimondo, A. R. Kolovsky, and A. Buchleitner, Nonlinearity induced destruction of resonant tunneling in the Wannier-Stark problem, Phys. Rev. A **72**, 063610 (2005).
[22] A. Zenesini, C. Sias, H. Lignier, Y. Singh, D. Ciampini, O. Morsch, R. Mannella, E. Arimondo, A. Tomadin, and S. Wimberger, Resonant tunneling of Bose-Einstein condensates in optical lattices, New J. Phys. **10**, 053038 (2008).
[23] K. Rapedius, C. Elsen, D. Witthaut, S. Wimberger, and H. J. Korsch, Nonlinear resonant tunneling of Bose-Einstein condensates in tilted optical lattices, Phys. Rev. A **82**, 063601 (2010).
[24] M. Glück, A. R. Kolovsky, and H. J. Korsch, Wannier-Stark resonances in optical and semiconductor superlattices, Phys. Rep. **366**, 103 (2002).